Inorganica Chimica Acta, 219 (1994) 127–133

Reactions of the polynuclear chain complex $[Cu(L)(H_2O)]_n$ (H_2L is 5-[(2′-carboxyphenyl)azo]-1,3-dimethylbarbituric acid) with imidazole. Crystal structures of the dinuclear and mononuclear derivatives and EPR study of the dimer–monomer equilibrium in solution

E. Colacio[a,*], J.M. Dominguez-Vera[a], R. Kivekäs[b], J.M. Moreno[a] and J. Ruiz[a]

[a]*Departamento de Química Inorgánica, Facultad de Ciencias, Universidad de Granada, 18071 Granada (Spain)*
[b]*Division of Inorganic Chemistry, University of Helsinki, PO Box 6, FIN-00014, Helsinki (Finland)*

(Received December 27, 1993)

Abstract

On treating the polynuclear chain complex $[Cu(L)(H_2O)]_n$ (H_2L is 5-[(2′-carboxyphenyl)azo]-1,3-dimethylbarbituric acid) with imidazole the complexes $[Cu(L)(Him)]_2$ (**1**) and $[Cu(L)(Him)_2]$ (**2**) are obtained. The structures of **1** and **2** have been determined by X-ray crystallographic methods. The structure of **1** consists of dinuclear units in which the copper ions are bridged by the barbituric ring. It crystallizes in the monoclinic space group $P2_1/c$ with cell constants $a=8.654(2)$, $b=22.64(2)$, $c=8.8048(8)$ Å, $\beta=103.76(1)°$, $Z=2$, $R=0.051$ and $R_w=0.041$. The structure of **2** consists of discrete $[Cu(L)(Him)_2]$ molecules held together by intermolecular hydrogen bonds to form infinite chains. It crystallizes in the triclinic space group $P\bar{1}$ with cell constants $a=8.268(2)$, $b=9.412(3)$, $c=13.798(5)$ Å, $\alpha=99.07(3)$, $\beta=91.20(3)$, $\gamma=108.64(2)°$, $Z=2$, $R=0.041$ and $R_w=0.035$. Comparison of the crystal structure of **1** with analogous complexes containing nitrogen heterocyclic ligands reveals that the replacement of imidazole by pyrazole or pyridine leads to very different crystal structures, which has been attributed to the different nature of the nitrogen heterocyclic ligand used in their syntheses. In dmso solution, EPR spectra of both complexes clearly indicate the existence of a monomer–dimer equilibrium.

Key words: Crystal structures; Copper complexes; Polydentate ligand complexes; Polynuclear complexes

Introduction

In previous papers [1–6], we have shown the versatility of different carboxyphenylazopyrimidine derivatives (Fig. 1) as ligands for the preparation of copper(II) complexes, ranging from mononuclear to infinite chains. Within the mononuclear fragment, coordination of the ligand occurs in a tridentate fashion through an exocyclic group of the pyrimidine ring, such as oxo or amino and N(8) and O(16) atoms belonging to the azo and carboxylate groups, respectively. Polynuclear metal complexes are formed by assembling the mononuclear units by two different types of bridges. In the first, the position of the carboxylate group in these polydentate ligands forces a *syn–anti* carboxylate bridge by coordination of the oxygen atom O(17) to a metal of an adjacent fragment, yielding di-, tri-, tetra-, hexa- and polynuclear chain copper complexes [1–4]. The second type of multiatom bridge, which is less usual than the former, occurs by coordination of an exocyclic oxo group from the pyrimidine ring to the metal ion of an adjacent unit [5]. Whatever multiatom bridge is present in these polynuclear complexes, the copper atoms adopt a (4+1) coordination mode. Four donors are afforded by the ligand, whereas the fifth coordination site is occupied by either a neutral molecule (water or nitrogen heterocyclic ligand) or an anion (nitrate or perchlorate).

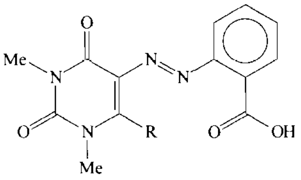

R= OH , NH_2 , $NHCH_3$

Fig. 1. Carboxyphenylazo derivatives used as ligands.

Central to these polynuclear complexes are their magnetic properties and, for those containing nitrogen

---

*Author to whom correspondence should be addressed.

SSDI 0020-1693(94)03838-F

heterocyclic ligands, the dimer–monomer equilibrium observed in solution. With regard to their magnetic behaviour, weak interactions, usually ferromagnetic, have been observed and explained on the basis of both the geometry around the copper(II) ions and the nature of the bridges. In this framework, we report here the preparation and the crystal structures of the complexes $[Cu(L)(Him)]_2$ and $[Cu(L)(Him)_2]$, in which the nitrogen heterocyclic ligand is imidazole (Him). These complexes are compared with those analogous containing pyridine and pyrazole [4, 5]. Furthermore, we wish to focus on the dimer–monomer equilibrium in solution, which has been characterized by EPR spectroscopy.

Experimental

Preparation of the compounds

The ligand H_2L was prepared according to the method described previously [7].

$[Cu(L)(Him)]_2$ (**1**) was prepared by dissolving $[Cu(L)(H_2O)]_n$ [2] (1.15 g, 3 mmol) in methanol and treating the resulting solution with the equimolecular amount of solid imidazole (0.2 g, 3 mmol). Slow evaporation of the resulting dark green solution yielded well developed black crystals, which were subsequently isolated by filtration, washed with methanol and air-dried. Yield 60%. *Anal.* Found: C, 44.3; H, 3.3; N, 19.3; Cu, 14.4. Calc. for $C_{32}H_{28}N_{12}O_{10}Cu_2$: C, 44.3; H, 3.2; N, 19.4; Cu, 14.6%. IR (KBr, cm^{-1}) 3060 ν(NH), 1713 ν(C(2)=O), 1656 ν(C(6)=O), 1573 $\nu_{asym}(CO_2)$, 1411 $\nu_{sym}(CO_2)$ and 1364 ν(N=N).

$[Cu(L)(Him)_2]$ (**2**) was prepared according to two different procedures. (i) The solid polynuclear compound $[Cu(L)(H_2O)]_n$ [2] (0.9 g, 2.4 mmol) was dissolved quickly in melted imidazole (1.0 g, 15 mmol) and the green mixture was stirred and treated with hot methanol. The resulting solution was allowed to stand for 2 days at room temperature, after which well developed green crystals of **2** formed. These were filtered off, washed with methanol and air-dried. (ii) An equimolecular amount of solid imidazole was added to a stirred solution of complex **1** in methanol. Yield 70%. *Anal.* Found: C, 45.3; H, 3.7; N, 22.2; Cu, 12.7. Calc. for $C_{19}H_{18}N_8O_5Cu$: C, 45.5; H, 3.6; N, 22.3; Cu, 12.7%. IR (KBr, cm^{-1}) 3242 ν(NH), 1707 ν(C(2)=O), 1630 ν(C(6)=O), 1582 $\nu_{asym}(CO_2)$, 1392 $\nu_{sym}(CO_2)$ and 1366 ν(N=N).

Physical measurements

Microanalyses of C, H and N, copper determination, IR and EPR spectra and the magnetic susceptibility data were obtained as already described [5].

X-ray data collection and structure determination

Single-crystal data collections were performed at 293 K on an automatic Nicolet P3F four-circle diffractometer using graphite monochromatized Mo Kα ($\lambda = 0.71069$ Å) radiation. Complex **1** crystallizes in the monoclinic system, space group $P2_1/c$ (No. 14), with $a = 8.654(2)$, $b = 22.64(2)$, $c = 8.8048(8)$ Å, $\beta = 103.76(1)°$, $U = 1675(2)$ Å^3, $Z = 2$, $D_c = 1.72$ g cm^{-3}, $F(000) = 884$ and μ(Mo Kα) $= 1.35$ mm^{-1}, crystal dimensions $0.13 \times 0.20 \times 0.28$ mm. Complex **2** crystallizes in the triclinic system, space group $P\bar{1}$ (No. 2), with $a = 8.268(2)$, $b = 9.412(3)$, $c = 13.798(5)$ Å, $\alpha = 99.07(3)$, $\beta = 91.20(3)$, $\gamma = 108.64(2)°$, $U = 1001.8(8)$ Å^3, $Z = 2$, $D_c = 1.66$ g cm^{-3}, $F(000) = 514$ and μ(Mo Kα) $= 1.14$ mm^{-1}, crystal dimensions $0.21 \times 0.28 \times 0.33$ mm.

The unit-cell parameters were calculated by least-squares refinements of 25 high angle independent reflections. The data were collected by ω–2θ scan mode ($3 < 2\theta < 55°$). Intensities of three standard reflections measured after every 60 reflections showed no significant intensity decrease during the course of the data collection. A total of 2307 and 3858 reflections was considered with $F > 3.0\sigma(F_o)$ and $F > 4.0\sigma(F_o)$, for **1** and **2**, respectively. Data for structure determinations were corrected for Lorentz and polarization effects, but not for absorption. The direct methods of the SHELXS [8] program were used to find the positions of the heavy atoms. Subsequent difference Fourier syntheses and least-squares refinements in the XTAL [9] package revealed the whole structures. In the final cycles the non-hydrogen atoms were refined anisotropically and the hydrogen atoms isotropically ($R = 0.051$, $R_w = 0.041$ and $R = 0.041$, $R_w = 0.035$ for **1** and **2**, respectively). Neutral atomic scattering and dispersion factors were those included in the XTAL program package. Atomic coordinates for the non-hydrogen atoms for both complexes are listed in Table 1. See also 'Supplementary material'.

Results and discussion

On reacting $[Cu(L)(H_2O)]_n$ with imidazole, and depending on the reaction conditions, the complexes $[Cu(L)(Him)]_2$ (**1**) and $[Cu(L)(Him)_2]$ (**2**) are obtained. Both complexes exhibit powder EPR spectra suggestive of some type of exchange interaction between the copper(II) ions. Furthermore, the EPR spectra in solution are indicative of a dimer–monomer equilibrium. Even though all these features are not totally unexpected in this kind of complex, given that the corresponding pyridine and pyrazole derivatives behave in a similar way, the X-ray crystal structure determinations reveal significant differences between them, which can be

TABLE 1. Non-hydrogen atomic fractional coordinates with e.s.d.s in parentheses and equivalent isotropic parameters for **1** and **2**

Atom	*x*/*a*	*y*/*b*	*z*/*c*	U_{eq} ^a^ (Å^2)	Atom	*x*/*a*	*y*/*b*	*z*/*c*	U_{eq} ^a^ (Å^2)
1					**2**				
Cu(1)	0.18997(8)	0.02339(3)	0.09886(8)	0.0329(2)	Cu(1)	0.12789(4)	0.59574(4)	0.33598(3)	0.0263(1)
O(2)	0.4186(5)	0.2037(2)	−0.3562(4)	0.050(2)	O(2)	−0.6254(2)	0.1134(2)	0.3167(2)	0.064(1)
O(4)	0.2533(4)	0.0936(1)	0.0034(4)	0.036(1)	O(4)	−0.1057(2)	0.4787(2)	0.3629(1)	0.0457(9)
O(6)	0.5594(4)	0.0105(1)	−0.3182(4)	0.042(1)	O(6)	−0.2215(2)	0.0429(2)	0.1143(1)	0.0486(9)
O(16)	0.0715(4)	−0.0384(1)	0.1674(4)	0.041(1)	O(16)	0.3717(2)	0.6917(2)	0.3528(1)	0.053(1)
O(17)	0.0563(5)	−0.1246(2)	0.2754(4)	0.048(1)	O(17)	0.6384(2)	0.7631(2)	0.3163(2)	0.074(1)
N(1)	0.4718(5)	0.1055(2)	−0.3532(5)	0.034(2)	N(1)	−0.4240(3)	0.0795(2)	0.2142(2)	0.042(1)
N(3)	0.3358(5)	0.1480(2)	−0.1775(5)	0.036(2)	N(3)	−0.3643(3)	0.2966(2)	0.3384(2)	0.040(1)
N(7)	0.3508(4)	−0.0129(2)	−0.1397(4)	0.026(1)	N(7)	0.0193(3)	0.2972(2)	0.2087(2)	0.036(1)
N(8)	0.2697(4)	−0.0294(2)	−0.0407(4)	0.028(1)	N(8)	0.1463(3)	0.4160(2)	0.2461(2)	0.036(1)
N(18)	0.1319(5)	0.0760(2)	0.2566(5)	0.034(2)	N(18)	0.1148(3)	0.7562(2)	0.4480(2)	0.042(1)
N(20)	0.0533(6)	0.1035(2)	0.4646(5)	0.046(2)	N(20)	0.1915(3)	0.9616(3)	0.5626(2)	0.049(1)
C(1)	0.5522(7)	0.1129(3)	−0.4823(7)	0.051(2)	C(1)	−0.5495(4)	−0.0609(3)	0.1603(2)	0.060(2)
C(2)	0.4089(6)	0.1557(2)	−0.3006(6)	0.035(2)	C(2)	−0.4810(3)	0.1594(3)	0.2910(2)	0.044(1)
C(3)	0.2743(8)	0.2014(2)	−0.1166(8)	0.059(3)	C(3)	−0.4263(4)	0.3846(3)	0.4187(2)	0.055(2)
C(4)	0.3165(6)	0.0948(2)	−0.1108(6)	0.031(2)	C(4)	−0.1976(3)	0.3542(3)	0.3147(2)	0.037(1)
C(5)	0.3747(6)	0.0435(2)	−0.1743(6)	0.028(2)	C(5)	−0.1411(3)	0.2657(3)	0.2372(2)	0.035(1)
C(6)	0.4758(6)	0.0503(2)	−0.2849(6)	0.032(2)	C(6)	−0.2584(3)	0.1240(3)	0.1834(2)	0.038(1)
C(9)	0.2602(6)	−0.0932(2)	−0.0356(6)	0.028(2)	C(9)	0.3007(3)	0.4143(3)	0.1977(2)	0.035(1)
C(10)	0.1873(6)	−0.1224(2)	0.0695(5)	0.028(2)	C(10)	0.4552(3)	0.5367(3)	0.2202(2)	0.039(1)
C(11)	0.1908(7)	−0.1840(2)	0.0717(6)	0.039(2)	C(11)	0.5951(3)	0.5293(3)	0.1653(2)	0.051(1)
C(12)	0.2557(7)	−0.2165(2)	−0.0283(7)	0.045(2)	C(12)	0.5853(4)	0.4088(4)	0.0927(2)	0.055(2)
C(13)	0.3251(7)	−0.1879(2)	−0.1326(6)	0.043(2)	C(13)	0.4353(4)	0.2876(3)	0.0736(2)	0.051(1)
C(14)	0.3270(6)	−0.1272(2)	−0.1367(6)	0.039(2)	C(14)	0.2953(3)	0.2901(3)	0.1259(2)	0.046(1)
C(15)	0.1010(6)	−0.0932(2)	0.1794(6)	0.032(2)	C(15)	0.4908(3)	0.6732(3)	0.3009(2)	0.044(1)
C(19)	0.0854(7)	0.0584(2)	0.3807(7)	0.052(3)	C(19)	0.2388(4)	0.8835(3)	0.4843(2)	0.049(1)
C(21)	0.0832(7)	0.1534(2)	0.3932(6)	0.047(2)	C(21)	0.0269(4)	0.8803(3)	0.5767(2)	0.053(1)
C(22)	0.1310(7)	0.1362(2)	0.2648(6)	0.044(2)	C(22)	−0.0196(4)	0.7550(3)	0.5060(2)	0.051(1)
					N(23)	0.0599(3)	0.6912(2)	0.2102(2)	0.041(1)
					C(24)	0.0020(4)	0.8074(3)	0.2175(2)	0.046(1)
					N(25)	−0.0189(3)	0.8442(3)	0.1293(2)	0.054(1)
					C(26)	0.0288(4)	0.7462(4)	0.0598(2)	0.053(2)
					C(27)	0.0760(4)	0.6534(3)	0.1111(2)	0.045(1)

^a^U_{eq} has been defined as $U_{eq}=1/3[\Sigma_i\Sigma_j U_{ij}(a^*_i\cdot a^*_j)(\mathbf{a}_i\cdot\mathbf{a}_j)]$.

attributed to the different nature of the nitrogen heterocyclic ligand used in their syntheses.

Crystal structure of 1

The structure of **1** consists of dinuclear [Cu(L)(Him)]$_2$ molecules with a C_i symmetry, in which the copper(II) ions are bridged by the barbituric ring with a Cu···Cu distance of 6.115(2) Å. A perspective view of the dinuclear unit is given in Fig. 2, while selected bond distances and angles are listed in Table 2.

Each copper(II) ion is in a (4+1) surrounding. The four nearest neighbours, at about 2.0 Å, are the O(4), N(8) and O(16) atoms from the double-deprotonated L ligand and the N(18) atom from imidazole. The fifth position is occupied by the O(6)^i atom (i=1−*x*, −*y*, −*z*) belonging to the barbituric ring of an adjacent and symmetry-related fragment, giving rise to the dinuclear compound.

The distortion of the five-coordinate complex from ideal square pyramidal and trigonal bipyramidal geometries has been calculated by using the τ index (τ is unity for trigonal bipyramid and zero for square-pyramid) introduced by Addison *et al.* [10]. The calculated τ value for **1** is 0.15, indicating that the CuN_2O_3 chromophore is close to square pyramidal geometry. The copper atom is not coplanar with the basal plane but lifted by 0.097(2) Å, as can be expected in a square pyramidal geometry [11].

It must be pointed out that coordination of the ligand through the oxygen atom O(6) of the pyrimidine ring to the copper atom of a neighbouring unit is quite unusual. This has only previously been observed in the polynuclear complexes [Cu$_4$(L^1)$_3$(HL^1)(NO$_3$)(H$_2$O)·2H$_2$O] (L^1 is the doubly deprotonated form of 6-amino-1,3-dimethyl-5-(2′-carboxyphenyl)azouracil) and [{Cu(L)(py)·3H$_2$O}$_n$], with Cu–O(6) distances of 2.31(2) and 2.462(4) Å, respectively [1, 5]. In this latter

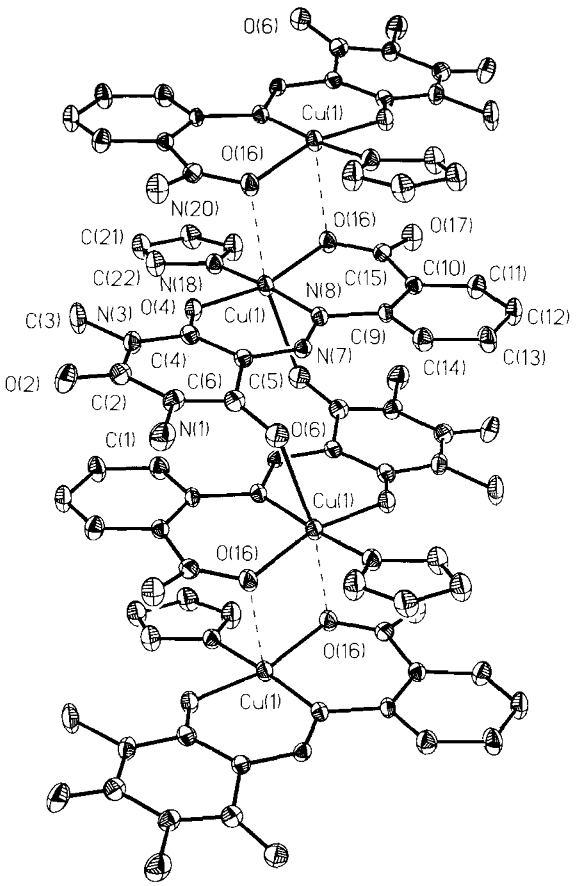

Fig. 2. A perspective view of complex **1**, parallel to the *a* axis.

TABLE 2. Selected bond distances (Å) and angles (°), with e.s.d.s in parentheses, for **1** and **2**

1		**2**	
Cu(1)–O(4)	1.937(4)	Cu(1)–O(4)	1.970(2)
Cu(1)–O(16)	1.914(4)	Cu(1)–O(16)	1.919(2)
Cu(1)–N(8)	1.954(4)	Cu(1)–N(8)	1.984(2)
Cu(1)–N(18)	1.983(4)	Cu(1)–N(18)	2.014(2)
Cu(1)–O(6)^i	2.651(3)	Cu(1)–N(23)	2.215(3)
O(16)–C(15)	1.266(6)	O(16)–C(15)	1.271(4)
O(17)–C(15)	1.235(7)	O(17)–C(15)	1.234(3)
N(7)–N(8)	1.298(6)	N(7)–N(8)	1.290(2)
O(4)–Cu(1)–O(16)	164.6(1)	O(4)–Cu(1)–O(16)	160.05(9)
O(4)–Cu(1)–N(8)	92.9(2)	O(4)–Cu(1)–N(8)	90.71(8)
O(4)–Cu(1)–N(18)	87.5(2)	O(4)–Cu(1)–N(18)	86.31(8)
O(16)–Cu(1)–N(8)	92.7(2)	O(16)–Cu(1)–N(8)	92.62(9)
O(16)–Cu(1)–N(18)	88.5(2)	O(16)–Cu(1)–N(18)	86.68(9)
N(8)–Cu(1)–N(18)	173.8(1)	N(8)–Cu(1)–N(18)	168.9(1)
O(6)^i–Cu(1)–O(4)	106.7(1)	N(23)–Cu(1)–O(4)	98.04(8)
O(6)^i–Cu(1)–N(8)	86.0(1)	N(23)–Cu(1)–O(16)	101.54(9)
O(6)^i–Cu(1)–O(16)	88.0(1)	N(23)–Cu(1)–N(18)	99.7(1)
O(6)^i–Cu(1)–N(18)	87.9(1)	N(23)–Cu(1)–N(8)	91.26(9)
O(16)–C(15)–O(17)	122.1(5)	O(16)–C(15)–O(17)	121.5(2)

$^i = 1-x, -y, -z$.

complex, the coordination of the ligand between mononuclear fragments is essentially similar to that observed in **1**, leading to the formation of a zig-zag chain instead of a dimer. This may be due to the existence of a hydrogen bond involving the imidazole molecule, which is not possible for pyridine.

On the other hand, the oxygen atom O(16) belonging to each carboxylate group of a dinuclear unit is located at 2.865(3) Å from the copper ion of an adjacent and centrosymmetrically related dinuclear unit (ii = $-x$, $-y$, $-z$), giving rise to a Cu···Cu^{ii} distance of 3.499(1) Å. The Cu–O(16)^{ii} distance is about 0.2 Å longer than those observed for weakly coordinated water or small anions but less than the sum of their van der Waals radii [11], indicating that, even though weak, some degree of bonding interaction exists between the dinuclear molecules. Taking this into account, the structure could be considered as a zig-zag chain of copper atoms parallel to the *a* axis, with two different Cu···Cu distances of 6.115(2) and 3.499(1) Å. A view of this chain is depicted in Fig. 2. Chains are interconnected by hydrogen bonds, each of these being established from the protonated nitrogen atom of the imidazole ring with the oxygen atom O(17) of a neighbouring molecule. The related donor–acceptor distance N(20)···O(17)^{iii} (iii = $-x$, $-y$, $1-z$) is 2.720(7) Å.

Comparison of the structures of **1**, [Cu(L)(Hpz)]$_2$ and [{Cu(L)(py)·3H$_2$O}$_n$] [4, 5] reveals that, even though numerous attempts to obtain iso-structural complexes have been made, the replacement of the nitrogen heterocyclic ligand yields a diversity of structures. This fact can only be explained by the presence or not of hydrogen bonds involving the nitrogen heterocyclic ligand. Thus, while hydrogen bonds are not possible for a coordinated pyridine, replacement of pyrazole by imidazole implies the existence of different intermolecular hydrogen bonds, which, ultimately, lead to different multiatom bridges between the copper atoms.

Crystal structure of 2

The structure of **2** consists of neutral [Cu(L)(Him)$_2$] molecules, held together by hydrogen bonds to form infinite chains. A perspective drawing of the complex is given in Fig. 3 together with the atomic labelling scheme. Selected bond lengths and angles are listed in Table 2.

As in **1**, the surrounding of the copper(II) ion is best described by a (4+1) square pyramidal geometry ($\tau = 0.15$). The basal plane is formed by the O(4), N(8) and O(16) atoms from L and N(18) from an imidazole molecule, whereas the apical position is occupied by the N(23) atom from a second imidazole ring. The maximum deviation of the atoms from the mean basal plane is 0.084(3) Å. As usual, the Cu(II) ion is lifted toward the axial donor by 0.267(1) Å [11]. Bond distances

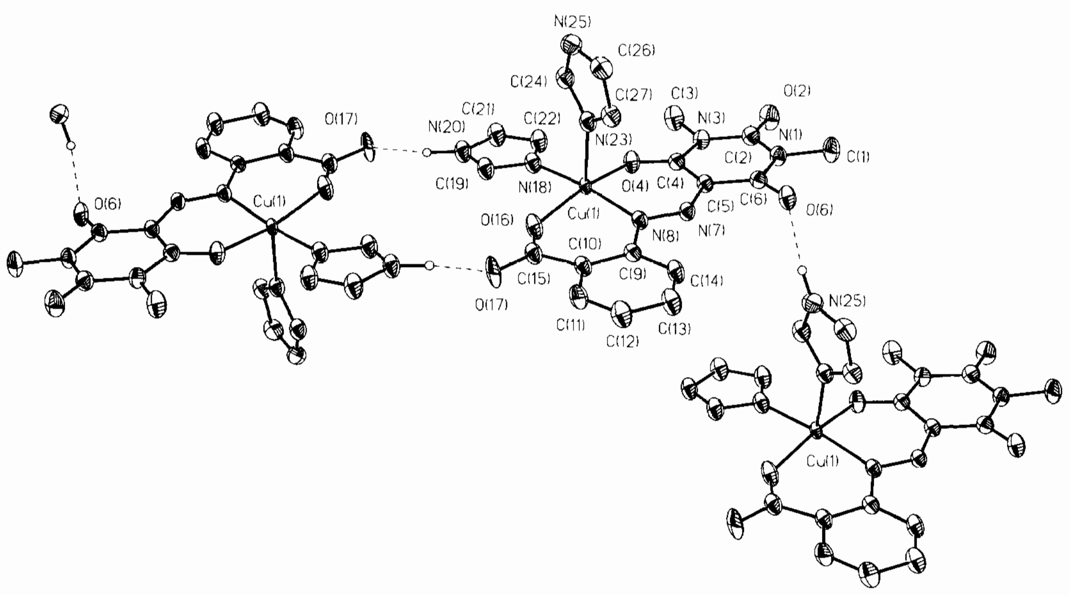

Fig. 3. A perspective view of complex **2**, including the H-bonding network.

in the basal plane range from 1.919(2) to 2.014(2) Å. They are shorter than the apical distance Cu–N(23) of 2.215(3) Å but slightly longer than those in complex **1**. Bond distances and angles in the tridentate ligand do not significantly differ from those found in **1**. The equatorial imidazole ring is close to being coplanar with the basal plane with a dihedral angle of 10.3(1)°. The mean planes of the equatorial and axial imidazole molecules form an angle of 84.7(1)° to each other. The shortest contact distance between these rings, N(18)· · ·N(23), is 3.235(3) Å, which is less than the sum of their van der Waals radii [12], indicating that some steric crowding remains in the structure.

Finally, the $[Cu(L)(Him)_2]$ molecules are held together by two different hydrogen bonds to form infinite chains (Fig. 3). The first involves the O(17) atom of the carboxylate group and the protonated $N(20)^{iv}$ atom ($iv=1-x$, $2-y$, $1-z$) of the equatorial imidazole belonging to a centrosymmetrically related neighbouring molecule with a donor–acceptor distance of 2.773(3) Å, forming a dinuclear unit with a Cu· · ·Cu distance of 8.620(2) Å. The second links these dinuclear units through the N(25) and $O(6)^{v}$ atoms ($v=x$, $1+y$, z), $N(25)\text{–}H\cdots O(6)^{v}=2.908(4)$ Å, leading to a zig-zag chain. Nevertheless, the shortest $Cu\cdots Cu^{vi}$ ($vi=-x$, $1-y$, $1-z$) distance of 5.361(2) Å occurs between non-hydrogen bonded molecules.

EPR study

Complexes **1** and **2** have quite similar polycrystalline EPR spectra in the 250–4 K temperature range. Both exhibit signals attributable to an axial doublet spectrum ($g_{\parallel}=2.20$ and $g_{\perp}=2.04$) and, at a high gain, the half-field signal $\Delta M=\pm 2$ ($g=4.00$ and 4.07 for **1** and **2**, respectively). Because these spectra were suggestive of magnetically coupled copper(II) centres, we decided to collect the magnetic susceptibility data on powdered samples in the range 250–2 K.

For **1**, the product $\chi_M T$ remains constant and equal to 0.40 cm^3 K mol^{-1} from 250 to 10 K and then slightly decreascs upon cooling down to 0.30 cm^3 K mol^{-1} at 2 K. The best fit to the Bleaney–Bowers equation [13] was found with $g=2.09$ and $2J=-0.91$ cm^{-1}. For **2**, the product $\chi_M T$ remains practically constant down to 4.4 K, indicating that $|2J|\leqslant 0.5$ cm^{-1}. The weak exchange interactions observed for **1** and **2** are consistent with the structural and electronic features of these complexes. Thus, in **1** the exchange pathways are very extended and furthermore the copper coordination polyhedra are oriented in such way that the overlap between the magnetic orbitals (mainly of $d_{x^2-y^2}$) is not efficient [5]. For **2**, the exchange pathways are also extended and involve either an axial position on the Cu(II) ion where the spin density of the unpaired electron is very small or a *syn–anti* carboxylate group, which, regardless of the magnetic orbital orientations, provide poor support for the propagation of the exchange interaction [2–6]. In view of all this, for both complexes, an overlap integral close to zero is expected and thus weak interactions [14].

Interestingly, in dmso solution at 90 K, complexes **1** and **2** exhibit essentially superimposable EPR spectra (Fig. 4(a)), with signals attributable to a triplet spectrum characteristic of two interacting copper(II) ions [14, 15] and to a doublet spectrum of a mononuclear species (see below), both coexisting in solution. As for the triplet, the half-field signal transition ($\Delta M=\pm 2$) appears as a seven-line hyperfine pattern at $g=4.2$ with

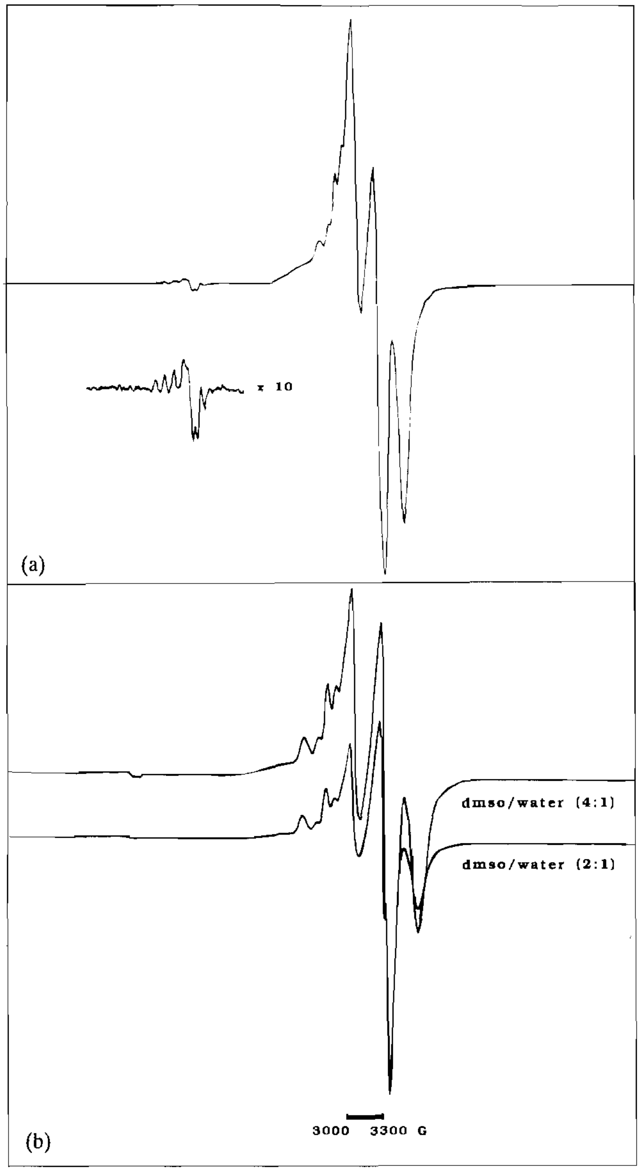

Fig. 4. (a) EPR spectrum of **1** and **2** in dmso solution at 90 K. (b) EPR spectrum of **1** and **2** in dmso/water solution at 90 K.

an average spacing of 63×10^{-4} cm^{-1}. The appearance of this pattern confirms the presence of a dinuclear complex in solution. In the 2750–2965 G region, four copper hyperfine lines can be observed with an average spacing of 65×10^{-4} cm^{-1}, which is almost equal to that of the half-field transition. The remaining three lines of this seven-line pattern could be located, one at high field, obscured by a strong signal at 3040 G, and two at low field, overlapping. These signals are assigned to the copper hyperfine splitting of one of the two five components of $g_{\parallel}$ [15, 16]. There should be another seven-line pattern resulting from the zero-field splitting at a much higher field position; however, none of them was located in the spectrum. They are likely obscured by the intense signal at 3500 G. Assuming an axial spectrum we may assign two signals at 3040 and 3500 G as $H_{x1} = H_{y1}$ and $H_{x2} = H_{y2}$, respectively, whereas the intense signal at 3260 G would be attributed to the $\Delta M = \pm 1$ transition of the mononuclear species. From the positions of the equatorial resonances, the zero-field splitting parameter D is estimated to be approximately equal to 0.05 cm^{-1}.

In order to determine if the hypothesis of two species coexisting in solution, giving rise to an axial spectrum for the dinuclear species, is consistent with our spectrum, we have carried out a study of the dependence of the spectrum on the water/dmso ratio. As can be observed from Fig. 4(b), the intensity of the signal at 3260 G increases as the water/dmso ratio is increased. This agrees with the existence of a monomer–dimer equilibrium, in which the presence of a more coordinating solvent, such as water, favours the formation of the mononuclear species. Moreover, addition of water modifies the spectrum in the 2750–2965 G region. Thus, the first and third lines, of the four previously observed, increase their intensity, by which they have been attributed to the hyperfine structure of $g_{\parallel}$ from the mononuclear species with an average spacing of 130×10^{-4} cm^{-1}. It should be noted that the copper hyperfine spacings of the $\Delta M = \pm 1$ and $\Delta M = \pm 2$ signals for the dinuclear complex are almost half that of the mononuclear complex responsible for the axial doublet spectrum, as expected for an exchange-coupled copper(II) dimer [17].

Conclusions

Reactions of $[Cu(L)(H_2O)]_n$ with nitrogen heterocyclic ligands such as pyridine, pyrazole and imidazole, depending on the reaction conditions, yield mononuclear and polynuclear copper(II) complexes. These latter exhibit two different multiatom bridges between the metal ions depending on the nature of the nitrogen heterocyclic ligand. In solution, both the mono- and polynuclear complexes show a similar monomer–dimer equilibrium, the mononuclear species being favoured by the use of coordinating solvents. With regard to the dinuclear species in solution, its formation would occur by assembling the mononuclear ones through the same bridges observed in the solid state. Nevertheless, more detailed studies are needed to determine if one of these bridges is favoured in solution.

Supplementary material

Tables of hydrogen atom coordinates, full listing of bond lengths and angles, anisotropic thermal parameters, least-squares plane equations, and observed and calculated structure factors are available from the authors on request.

Acknowledgements

The authors are grateful to DGCYT for the project of investigation PB88-0482 and to the Junta of Andalucía for financial support.

References

1 E. Colacio, J.P. Costes, R. Kivekäs, J.P. Laurent and J. Ruiz, *Inorg. Chem., 29* (1990) 4240.

2 E. Colacio, J.M. Dominguez-Vera, J.P. Costes, R. Kivekäs, J.P. Laurent, J. Ruiz and M. Sundberg, *Inorg. Chem., 31* (1992) 774.

3 E. Colacio, J.M. Dominguez-Vera, R. Kivekäs, J.M. Moreno, A. Romerosa and J. Ruiz, *Inorg. Chim. Acta, 212* (1993) 115.

4 E. Colacio, J.M. Dominguez-Vera, R. Kivekäs and J. Ruiz, *Inorg. Chim. Acta, 218* (1994) 109.

5 E. Colacio, J. Ruiz, J.M. Moreno, R. Kivekäs, M.R. Sundberg, J.M. Dominguez-Vera and J.P. Laurent, *J. Chem. Soc., Dalton Trans.,* (1993) 157, and refs. therein.

6 J.M. Moreno, J. Ruiz, J.M. Dominguez-Vera and E. Colacio, *Inorg. Chim. Acta, 208* (1993) 111.

7 M.S. Masoud, S.A. Abou Ali, G.Y. Ali and I.M. Abed, *Thermochim. Acta, 122* (1987) 209.

8 G.M. Sheldrick, *SHELXS 86,* program for solution of crystal structure, University of Göttingen, Germany, 1986.

9 S.R. Hall and J.M. Stewart (eds.), *XTAL 2.6. User's Manual,* Universities of Western Australia and Maryland, 1989.

10 A.W. Addison, T. Nageswara Rao, J. Reedijk, J. van Rijn and G.C. Verschoor, *J. Chem. Soc., Dalton Trans.,* (1984) 1349.

11 B.J. Hathaway, *Struct. Bonding (Berlin), 57* (1984) 55.

12 J.E. Huheey, *Inorganic Chemistry,* Harper International, New York, 3rd edn., 1983, pp. 258–259.

13 B. Bleaney and K.D. Bowers, *Proc. R. Soc. London, Ser. A, 214* (1952) 451.

14 O. Khan, in D. Gatteschi, O. Khan and R.D. Willett (eds.), *Magneto-Structural Correlations in Exchange Coupled Systems,* Reidel, Dordrecht, Netherlands, 1985.

15 J.P. Costes, F. Dahan and J.P. Laurent, *Inorg. Chem., 24* (1985) 1018.

16 A. Bencini, D. Gatteschi, C. Zanchini, J.G. Haasnoot, R. Prins and J. Reedijk, *Inorg. Chem., 24* (1985) 2812.

17 T.R. Felthouse and D.N. Hendrickson, *Inorg. Chem., 17* (1978) 444.